https://github.com/StuartsProjects/SX12XX-LoRa

https://jgromes.github.io/RadioLib/class_s_x1280.html

Application Note:

An Introduction to Ranging with the SX1280 Transceiver

AN1200.29
Rev 1.0
March 2017

Table of Contents

List of Figures

1 Basic Operation

The ranging functionality of SX1280 is based upon the measurement of a round trip time of flight between a pair of SX1280 transceivers. This process uses the LoRa modulation scheme so the ranging benefits from all of the advantages of long range and operation at low consumption conferred by LoRa. The basic ranging operation is outlined in the sequence below:

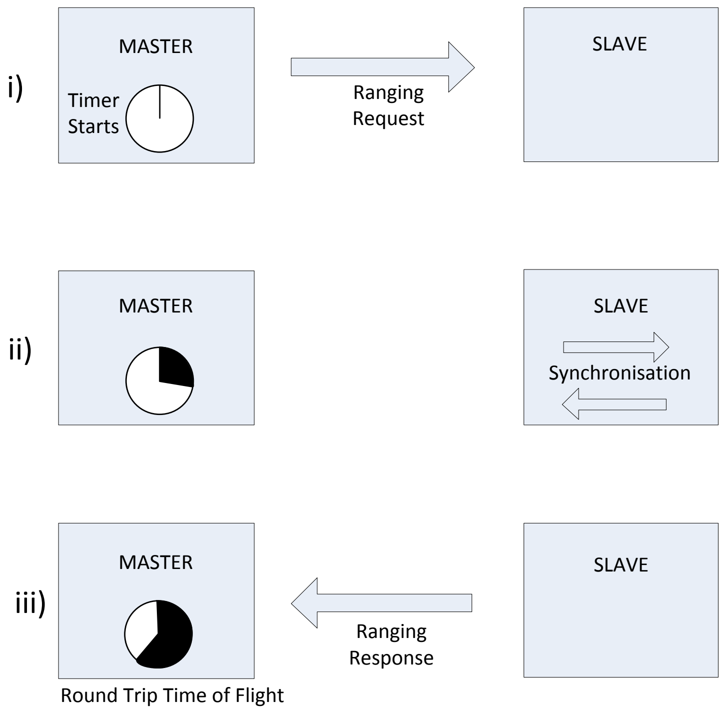

Slave must be ready to listen

Figure 1: Time of Flight Measurement Process

i) One SX1280 assumes the role of Master and initiates a ranging exchange by transmission of a ranging request. The ranging request is addressed to another SX1280, which must be configured in ranging Slave mode, so ready to receive the incoming ranging request. At the moment that the Master sends the ranging request, it also starts an internal timer.

ii) The ranging request is received by the addressed Slave, which synchronizes itself with the incoming signal. The Slave does not know at which time the signal was set, but the synchronization process requires a fixed amount of time known by the Master. Master and Slave never share a common absolute timing reference.

iii) Finally the Slave sends the synchronized ranging response back to the Master, upon reception of which the Master can deduce the round-trip time of flight from the time elapsed i.e. the time taken for the electromagnetic wave to propagate from Master to Slave and back again.

2 Source of Ranging Error

2.1 Measurement Error and Dilution of Precision

The principal sources of measurement error are outlined in the more detailed depiction of the Master and Slave below, here we see both of the radios involved in the ranging exchange. Each potential source of error is itemized below. Note that although the subscripts refer only to the Master, the same errors also affect the Slave.

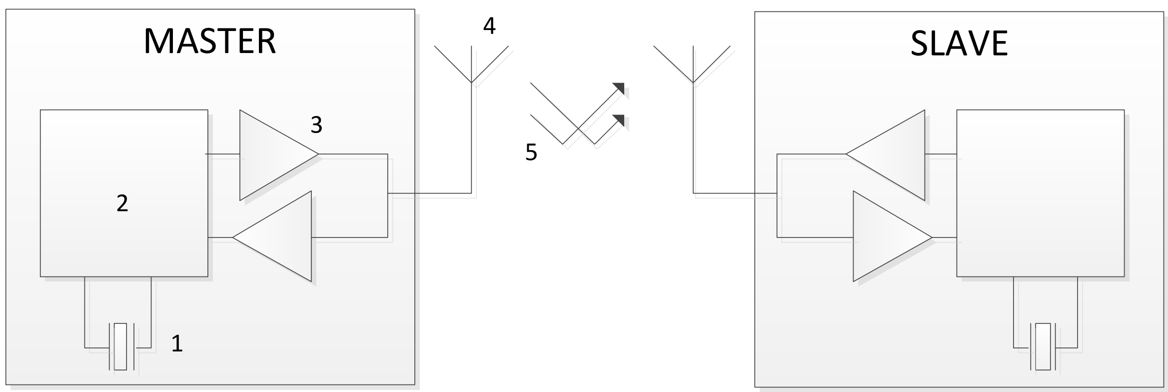

Figure 2: Sources of RTToF Ranging Error

Variable due to drift

As we saw in the previous section the Master generates a local clock that is used to time the round trip time of flight (RTToF) based upon the synchronized ranging response from the Slave. A known delay is incurred as the Slave synchronizes to the Master. If the precise clock frequency of the Slave differs from that of the Master then an unknown timing, so equivalently distance, offset is incurred. This source of this error is known as crystal timing error (1).

Fixed as No drift

Further delay (or distance) error is accumulated through transmit and receive paths of the radio as signals propagate through both digital (2) and analogue (3) signal processing and conditioning blocks. Ordinarily such delays can be considered design specific, meaning that this delay must be known for a given design to be compensated.

Fixed

Another similar source of measurement error is the antenna delay (4). Wherein a signal radiated (or by reciprocity received) by the antenna will experience a certain delay. Moreover, such a delay may not be uniform, in the sense that the delay experienced in one direction of radiation may differ from that of another direction.

It is important to differentiate between factors that affect the time of flight measurement accuracy and external environmental influences that might dilute that measurement precision. Multipath (5) is the phenomenon by which the radiated electromagnetic wave will take multiple reflected and diffracted paths from transmitter to receiver. Although compensation of multipath effects is beyond the scope of this Note, it is important to understand that this effect becomes more severe where there are obstructions between transmitter and receiver [1].

In this Application Note we will therefore not consider multipath (5) and the influence of the antenna (4) on the overall accuracy. By considering measurement performance in somewhat ideal Line-of-Sight (LoS) conditions, and not the external environmental factors that might dilute the ranging accuracy or precision, we will aim to reveal the underlying SX1280 ranging performance. In so doing, we can improve the accuracy of the range measurement system independent of both end-application and specific design implementation.

In summary, based upon this partition of the various sources of error, we can conclude that we are faced with compensation of the following two kinds of error:

- A **fixed** offset due to the various specific delays is to be compensated
- An unknown **variable** reference timing offset between Master and Slave is to be corrected.

In *Section 3* and *Section 4* of this Note we will concentrate on compensation of the sources of measurement error identified above. In *Section 5* we will discuss the difference between accuracy and precision. Then in *Section 6* and *Section 7* we will go on to detail the resulting measurement accuracy that is possible with the ranging functionality of SX1280 in an ideal channel and a line of sight channel respectively. *Section 8* deals with ranging measurements performed at short range before summarizing our conclusions in *Section 9*.

Variable: Error changes with time

3 Correction of Fixed Delays

3.1 Elimination of Timing Error

Acknowledging that the timing and frequency offset between Master and Slave can cause time varying ranging estimation errors, the question arises of how to apply a universal correction for the intrinsic delay of a given design in the presence of an unknown time varying error.

The answer is to characterize the ranging channel in such a way that the timing error is cancelled. Techniques for such a correction are well known [2]. In our case, this is done by switching the roles of ranging Master and ranging Slave. The principle is outlined below:

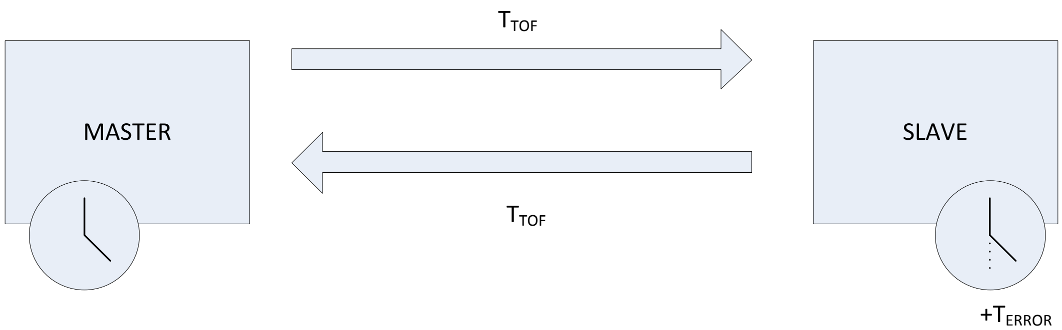

Figure 3: Master and Slave switching

In the first image we see that a timing error between the clocks of the two units of $+T_{ERROR}$ produces a ranging (timing) measurement that will include this error.

$$T_{Master-Slave} = 2T_{ToF} + T_{ERROR}$$

However if we reverse the roles of the two units (Master becomes Slave and vice versa). Then the sign of the timing error is also reversed. From this reverse perspective:

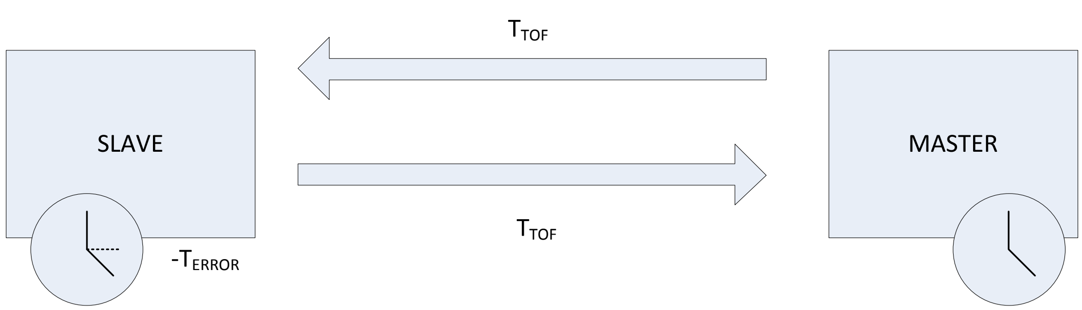

Figure 4: Master and Slave switching with Timing Error

$$T_{Slave-Master} = 2T_{ToF} - T_{ERROR}$$

Thus if we take the average of both measurements, then the resultant range (timing) figure is representative of the true distance, with the timing error being cancelled. Trivially:

$$T_{RTToF} = \frac{T_{Slave-Master} + T_{Master-Slave}}{2}$$

This approach assumes that any timing drift between Master and Slave is negligible for the timescale over which the measurement is performed. The principal source of timing reference drift is due to fluctuations in temperature causing the crystal reference oscillator of the SX1280 to drift. Provided measurements are performed at equivalent temperature, we can therefore consider the oscillator drift to be static. This means that this technique will cancel the timing offset error.

3.2 Practical Ranging Calibration Measurements

The figure below is a simplified block schematic of a conducted ranging measurement setup. The objective of such a measurement is to characterize the fixed design-specific delay, so that it can be calibrated out. Note the modification of the design for SMA connectors, the addition of RF attenuator in the signal path and the use of a pair of shielded enclosures to negate the influence of the shorter direct radiated path between the boards.

A known electrical length of coaxial cable (HCAAY 50-12) is used as it provides a known time delay (or equivalently electrical distance) between Master and Slave and a single path without multipath reflections. Any coaxial cable can be used.

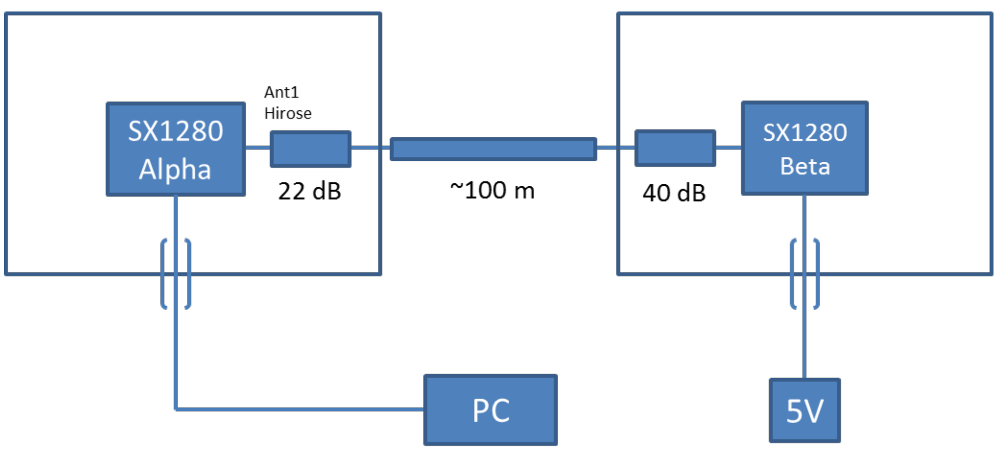

Figure 5: Schematic of the Calibration Measurement Setup

As stated in the previous section, it is important to minimize drift between the two sequences of role reversed measurements. We do so by ensuring the same operating temperature during role swapping to reduce the crystal drift.

Due to the statistical spread of the ranging results, it is necessary to perform the calibration measurements over a wide range of frequencies (which should cover the band of interest) and consider the average of multiple results.

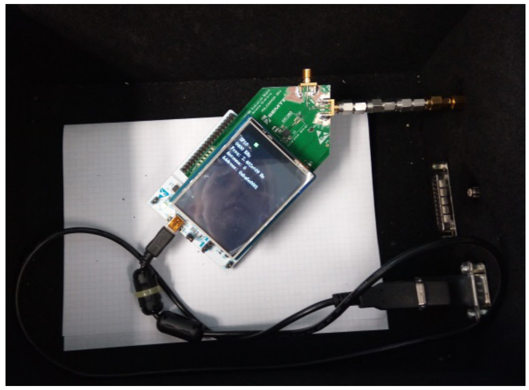

Figure 6: Screened Reference Design Modified for Cabled Use

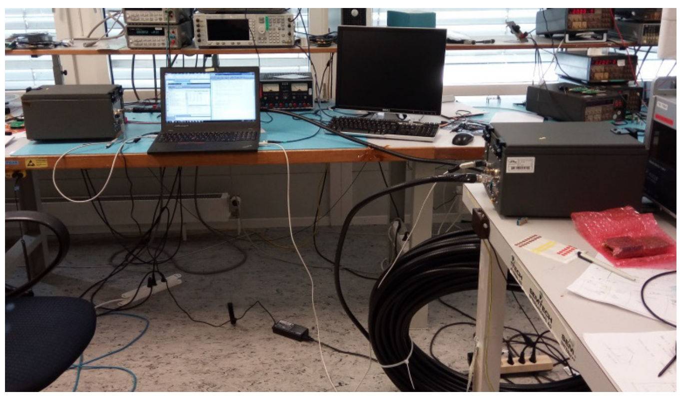

Figure 7: Actual Measurement Setup

In this test 500 measurement results were taken over 40 channels covering the 2.4 GHz ISM band. Following the timing offset cancellation method introduced in *Section 3.1*, the ranging calibration compensation can now be calculated as a simple additive timing offset as shown below.

The distance resolution of a given modem configuration - corresponding to one LSB of ranging resolution, D_{LSB}, in meters is given by:

$$D_{LSB} = \frac{c}{2^{12}\,BW}$$

Where BW is the programmed modulation bandwidth in Hz and c is the speed of light. It is very important to note the difference between resolution and accuracy. Whilst the resolution of the measurement may be very high, this does not imply the possibility of accuracy to this level.

To convert the raw output register output, *RangingResult*, to an RTToF distance (i.e. round trip distance) the following conversion should be used:

$$D_{RTToF} = RangingResult\ D_{LSB}$$

With this knowledge, the averaged *RangingResult* can then be used to calculate the calibration values.

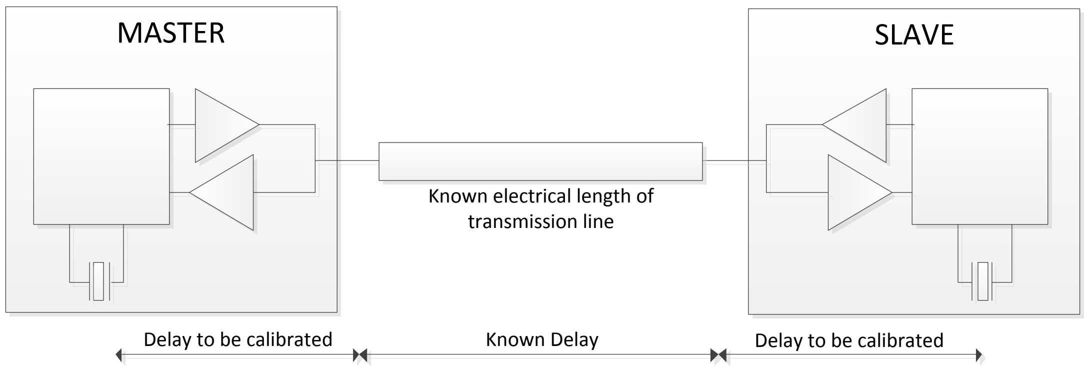

Figure 8: Ranging Setup

This is illustrated in the figure above (omitting the role swapping for clarity). The averaged output of each pair of round trip time of flight measurements will incur the delays outlined above twice.

Assuming both Master and Slave employ the same hardware design and a known electrical length of cable D_{cable} is used, then the calibration value is simply:

$$D_{uncalibrated} = (RangingResult * D_{LSB})/2$$

$$D_{calibration} = (D_{uncalibrated} - D_{cable}) / 2$$

$$Calibration = D_{calibration} / D_{LSB}$$

3.3 Calibration of Design Specific Delays

The following calibration table was assembled using the Master/Slave role reversal technique and calculated, as detailed above, from 500 ranging measurements at 40 channels across the 2.4 GHz ISM band (between 2402 MHz, 2480 MHz). Note that ranging operation with SX1280 is limited to the range of bandwidths from 400 kHz to 1.6 MHz and spreading factors SF5 to SF10.

Table 1: Measured Calibration Values

		SF					
		5	**6**	**7**	**8**	**9**	**10**
BW (kHz)	**400**	10299	10271	10244	10242	10230	10246
	800	11486	11474	11453	11426	11417	11401
	1600	13308	13493	13528	13515	13430	13376

Once these values are known for a given design, the process of applying the calibration correction is fully automated in SX1280. The calibration value must simply be written to the *RxTxDelay* register for the correction to be applied automatically. Please refer to the SX1280 datasheet [3] for more details.

3.4 Aside: Bidirectional Ranging Protocol

It should be noted that we could use this role reversal between Master and Slave as the basis for a ranging communication protocol that cancels the reference timing error. In legacy ranging systems such techniques have historically been employed [2].

However, this implies a doubling of our communication overhead to cancel the timing error. Transmission is the highest energy consumption activity the radio can engage in. Other techniques that do not incur this consumption penalty are preferred and are discussed in *Section 4.3*.

4 Correction of Timing Errors

With the fixed and design-specific delays calibrated, the major potential remaining source of error is the clock offset between Master and Slave. The same external crystal oscillator is used as the reference for both the ranging distance measurement process and to derive the RF carrier frequency of the SX1280. Because of this, a measurement of carrier frequency corresponds to a measurement of the timing drift between Master and Slave.

4.1 Characterization

The curves below show the influence of timing drift offset between Master and Slave on the raw ranging distance evaluation for the worst case 400 kHz bandwidth setting. Here we see that the distance error worsens with increasing SF and timing drift (so equivalently carrier frequency offset) between Master and Slave. The range error presented here corresponds to the ± 30 ppm range over which LoRa communication, so ranging, is possible.

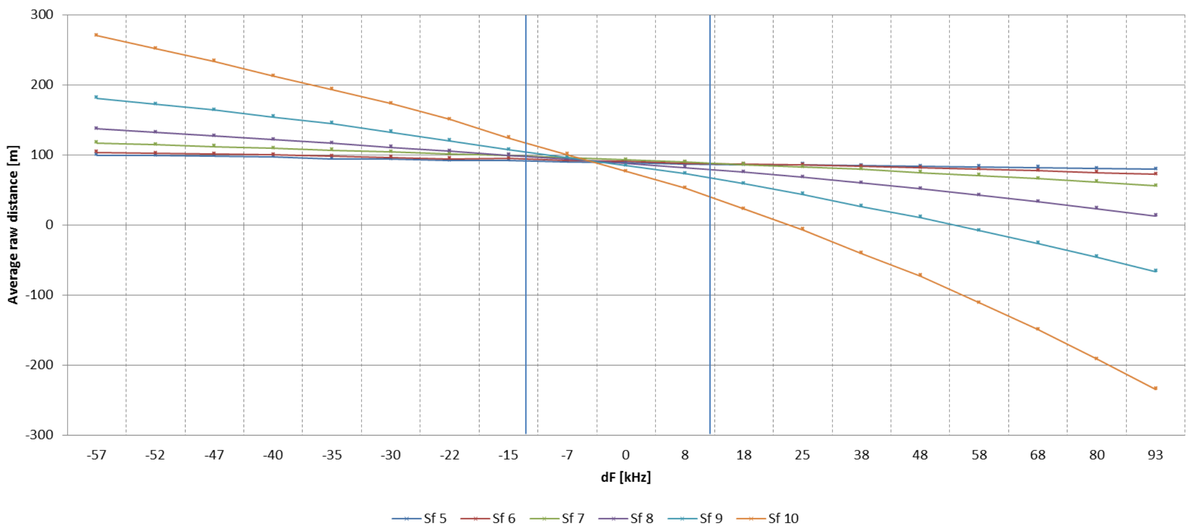

Figure 9: Distance Error as Function of Frequency Offset between Master and Slave (400 kHz BW)

The distance offset is not linear, especially at higher spreading factors. Initial correction of the frequency error, therefore relies on two facets:

1) Reduction of the range of error by using higher precision oscillator

2) Piecewise linear distance error correction

Because the RF signal and the timing reference for the ranging synchronization operation are the same crystal reference oscillator, a simple frequency error measurement of the frequency error between Master and Slave, using the LoRa Frequency Error Indicator (FEI), can be used to accurately evaluate the timing, and equivalently distance, error.

4.2 Correction

Using a linear correction, the corrected range measurement is calculated as:

$$Range' = Range - (m\ f_{error})$$

where f_{error} is the measured frequency error in kHz and m is the gradient correction taken from the characterization measurements of Section 4.1 and summarized in the table below. Recall that ranging operation with SX1280 is limited to the range of bandwidths from 400 kHz to 1.6 MHz and spreading factors SF5 to SF10.

Table 2: Frequency to Distance Error Gradient

m		SF					
		5	6	7	8	9	10
BW (kHz)	400	-0.148	-0.214	-0.419	-0.853	-1.686	-3.423
	800	-0.041	-0.118	-0.218	-0.429	-0.853	-1.737
	1600	0.103	-0.041	-0.101	-0.211	-0.424	-0.87

4.3 Protocol Implications

Because of the need to measure the frequency error, employing this technique practically infers the use of a standard LoRa communication prior to the ranging exchange itself. This can be useful as no payload data can be carried within the ranging frame, so may be useful for authentication purposes or transferring application payload data.

Note that such communication frames incur a much lower overhead of communication than the bidirectional approach [2]. This is because a frequency measurement is repeated only during the timescale over which a significant crystal frequency change may occur. In practical testing 40 ranging exchanges for a single LoRa communication packet for frequency measurement have proved successful.

It is not clear, how frequently these 40 ranging exchanges were taken

5 Accuracy and Precision

Before we go on to evaluate the accuracy of a given calibration, it is first necessary to define how we quantify accuracy. Below we borrow the definitions of accuracy and precision defined by Bartlett [4] and apply them to our ranging measurement scenario.

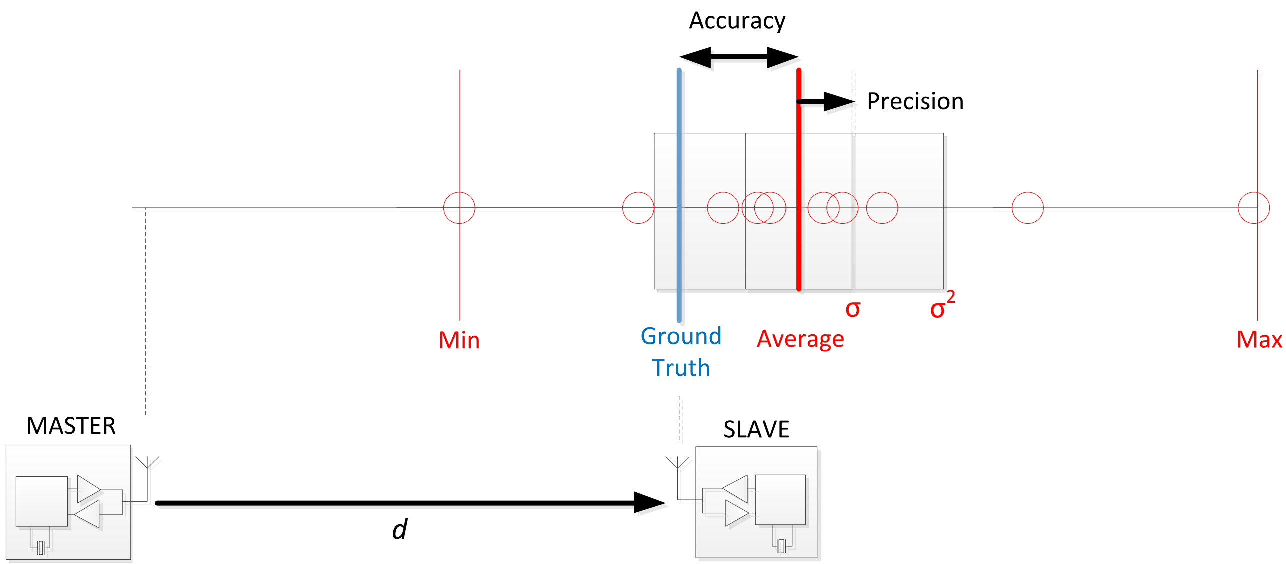

Figure 10: Illustration of the Principle of Accuracy and Precision

Here we see a Master and Slave unit located at physical distance, *d*, from one another. The actual physical location of the Slave is known as Ground Truth (shown in blue above). Each red circle represents the result of a single range measurement. The scales are exaggerated here for clarity.

Statistical quantities are calculated over the range of measurement values and are illustrated above. The resulting distance offset between the average and ground truth is the ranging **accuracy**.

Precision is a measure of the spread of the results. Various definitions of the precision are possible, in our case however, we define the ranging precision as standard deviation of the measurement values.

With this understanding of the difference between ranging accuracy and precision we can now go on to examine the theoretical performance of the ranging system and compare it with real measurements in both ideal and practical ranging scenarios.

6 Ranging Precision in an Ideal Channel

6.1 Theoretical Precision

The accuracy of the ranging measurement in an ideal environment (not disrupted by propagation effects such as reflected or diffracted paths that might artificially lengthen the measured range) will be governed by the accuracy of the calibration correction applied to the radio.

What about the precision? Although a few interpretations are available, based upon the method presented in [5] we calculate the Cramér Rao Lower Bound (CRLB) for the precision of a spread spectrum RTToF system as:

$$\sigma^2 = \frac{1}{8\pi^2 \; SNR \; \sqrt{N} \; BW \; 2^{SF}}$$

where SNR is the linear signal to noise ratio of the received signal, N is the number of ranging symbols (20 in our case), BW is the signal bandwidth and SF is the LoRa spreading factor.

Whilst practically generating a signal with a *specific* SNR over the air isn't easy, it is nevertheless highly informative to plot the CRLB as a function of the modulation parameters available in SX1280. Remaining with our original objective of evaluating the ranging performance under favorable channel conditions, we consider the CRLB with a positive SNR of+10 dB and plot this below.

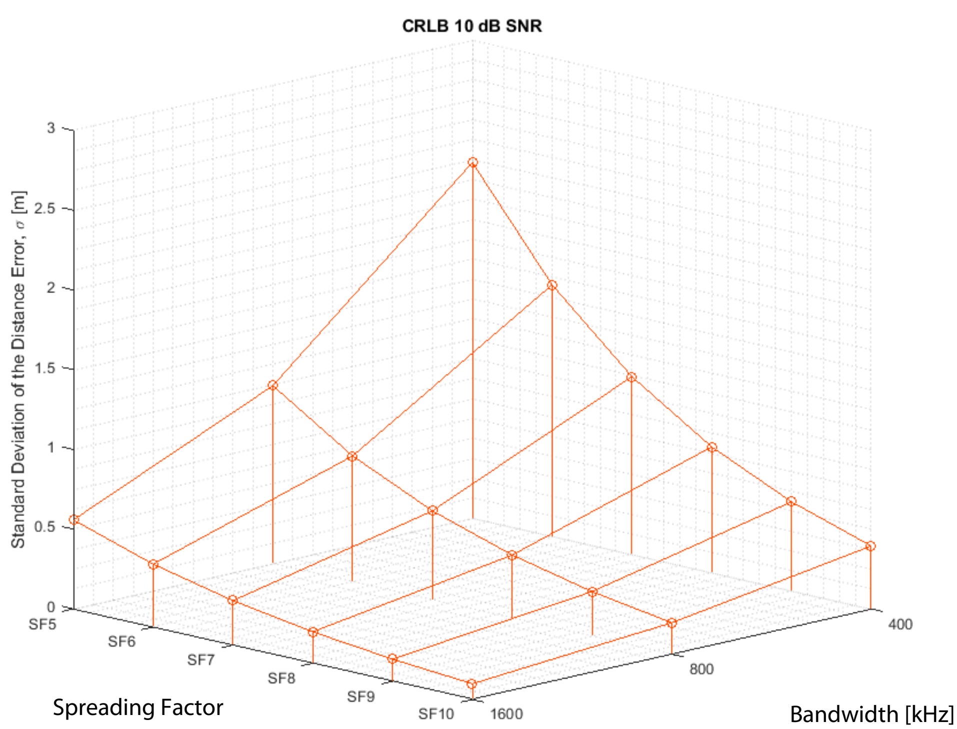

Figure 11: CRLB with SNR = 10 dB

Here we see how the standard deviation of the range measurement error σ (on the vertical axis) varies as a function of the modulation settings available in the SX1280 ranging engine. Spreading factor is on the leftmost axis and modulation bandwidth on the right hand axis.

The higher bandwidth improves the temporal resolution of the measurement and the higher spreading factor increases the integration time. The influence on the ranging precision is clear, for equivalent SNR, it shows a marked improvement in precision is possible by progressing to higher spreading factor and higher bandwidth.

6.2 Measured Precision

To simulate an ideal channel we employ a 108-meter length of coaxial cable (equivalent to an electrical length of ~123 m) using the same measurement setup as in *Section 3*. The result below is based upon 500 individual raw ranging exchanges, in the highest precision measurement channel in the ISM band. Measured SNR was measured in the range of +7 to +11 dB. Here we see performance at low bandwidth and low SF that approaches the bounded performance.

Generally, increasing SF and bandwidth improve the precision – but to a lesser extent than that of the CRLB. The principle difference, however, is that the precision attains a marginally lower minimum at SF9 rather than SF10. The optimal performance is realized at a bandwidth of 1600 kHz with a precision of 0.42 m ~~RMS~~ ranging error.

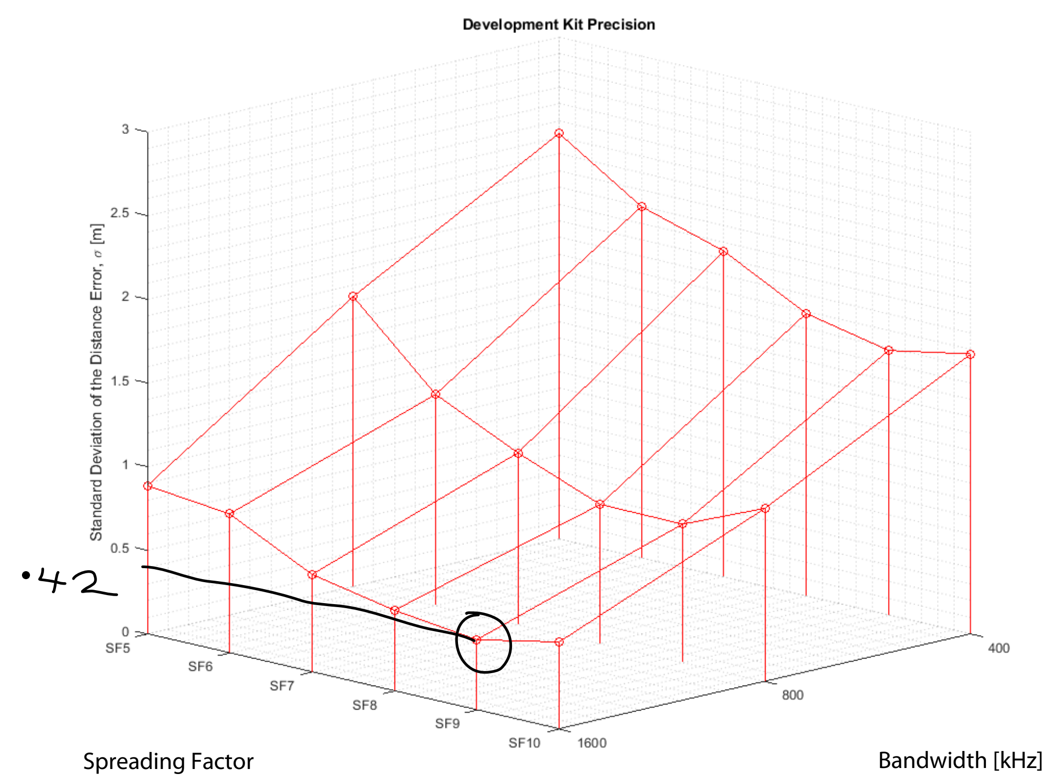

Figure 12: Single Channel Measured Precision of SX1280 Ranging in Cable

6.3 Ranging Protocol Considerations

Before introducing the ranging results obtained over-the-air, this section details the ranging protocol implemented, as it influences the overall ranging accuracy and precision.

For our experimental setup we use the Bluetooth Low Energy channel plan comprising 40 channels from 2402 MHz to 2480 MHz. The radio performs a single LoRa communication exchange on a fixed channel prior to each hopped measurement sequence from which the received signal strength and frequency error are determined. Then all 40 channels are randomly hoped over with a single ranging exchange between Master and Slave performed on each one.

Although potentially impractical in some applications, this entire process is repeated 50 times to gather a statistically significant sample size. Hence a total of 2000 measurements are performed in total. The limitations and proposals for a practical system are addressed after the measurement results in *Section 7.5*.

7 Ranging Precision in a Line of Sight Channel

With the basic ranging protocol described in *Section 6.3* established, it is possible to conduct initial outdoor line of sight evaluation of the SX1280 ranging functionality.

7.1 Precision Measurement Setup

In the line of sight range test the ranging Master is deployed 171.2 m from the Slave, both mounted at a height of 1.8 m from the ground with clear, optical, line of sight between both units and negligible clutter due to the defoliated vegetation at ground level.

NB: although depicted in snow, experiments were performed in a variety of climatic conditions with no measureable influence.

With the test setup established 500 ranging exchanges were performed over the same 40 channels as detailed in the previous section.

Figure 13: Ranging Test Site
Left: Ranging Slave, view towards Master
Right: Ranging Master view towards Slave

7.2 Precision Measurement Results

The results of the measurements performed at 170 m are shown below. The results are based upon 50 frequency-hopped ranging exchanges over 40 channels, from which the best channel is selected and the precision calculated for comparison with the ideal (cable) channel.

Here we see that at the highest spreading factor and bandwidth combination, we obtain approximately 1 m of RMS ranging precision. This corresponds to a dilution of precision of a factor of roughly 2 to 2.5 compared with the ideal (coaxial cable) channel.

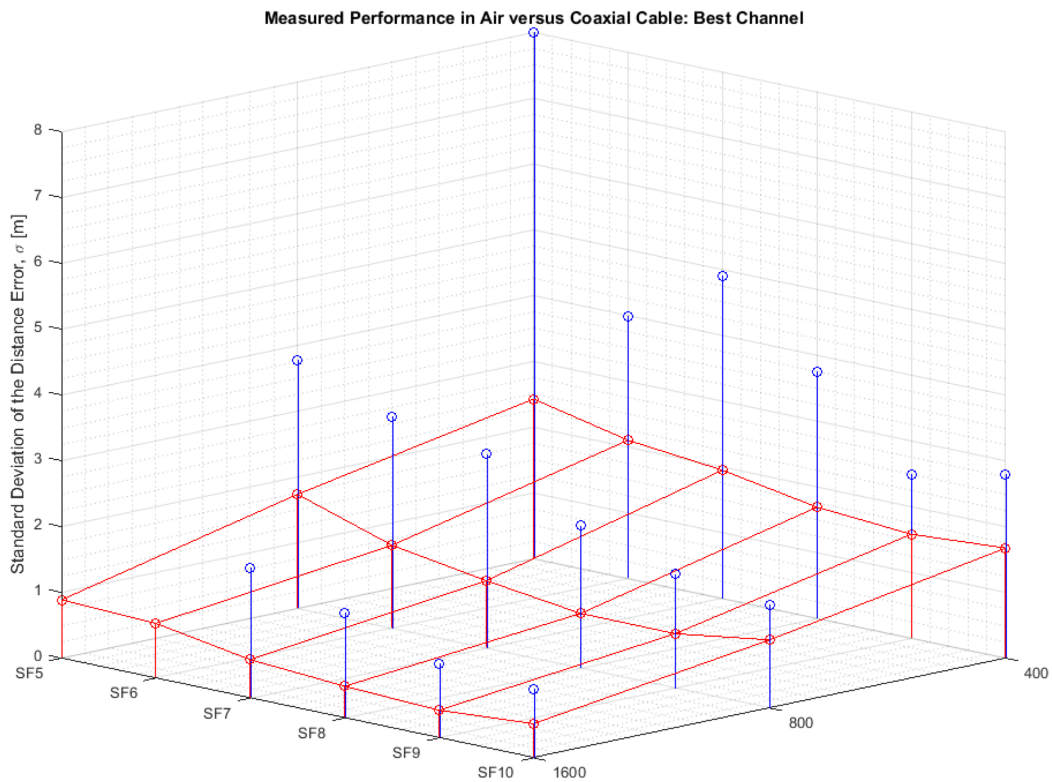

Figure 14: Measured Line-of-Sight Ranging Precision Compared with Cable

7.3 Accuracy Measurement Setup

For a thorough investigation of the accuracy, the measurement process of the preceding section was repeated at several ranges between 10 and 200 m in a line-of-sight environment. The measurement setup is shown below. Here each range, determined by GPS, is validated by a laser range finder [6].

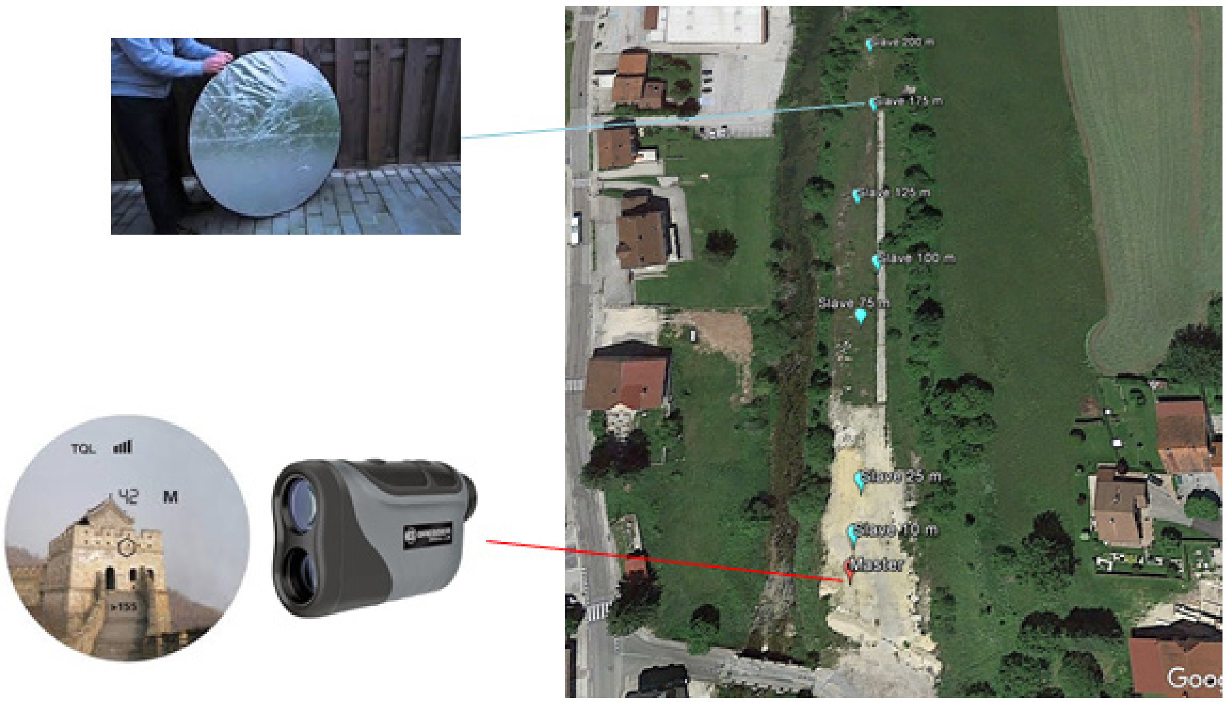

Figure 15: Experimental Setup for Ranging Accuracy Measurement as Function of Distance

To get laser distance measurements at distances of 200 m it is necessary to use a reflector, so a 1-meter diameter photographic reflector was used as a target. Nonetheless, at 200 m the reflector is smaller than the sight reticle of the range finder [6]. Consequently, some inconsistency in range finder results was noted.

Interestingly the laser range finder selected has a measurement display resolution of +/-1 m, based upon the empirical work done in [7] we conservatively estimate the operator error as 2% of the overall range. Thus the overall measurement error is as shown in the figure below.

At its highest value, the error of the laser range finder at 200 m is estimated as 5 m.

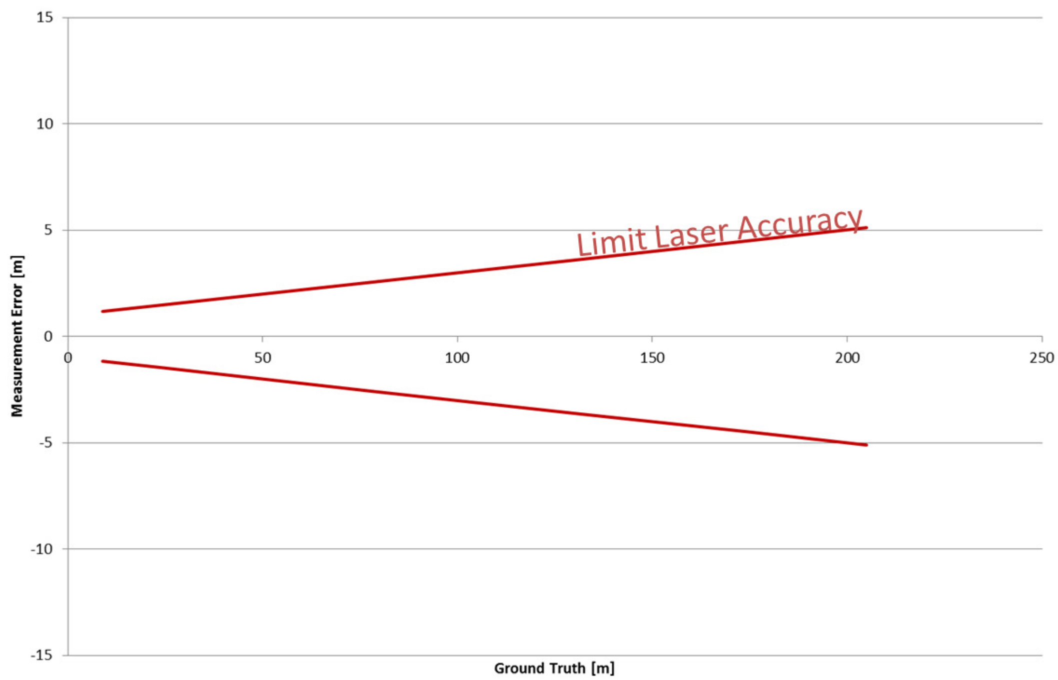

Figure 16: Theoretical Measurement Accuracy of Laser Range Finder Based upon 2% Operator Error

7.4 Accuracy Measurement Results

The accuracy measurements of the SX1280 are detailed in the following figures - each point corresponds to the average of the 2000 RTToF measurements. At 400 kHz measurement bandwidth, RTToF measurements are at the same order of magnitude as the laser range finder error:

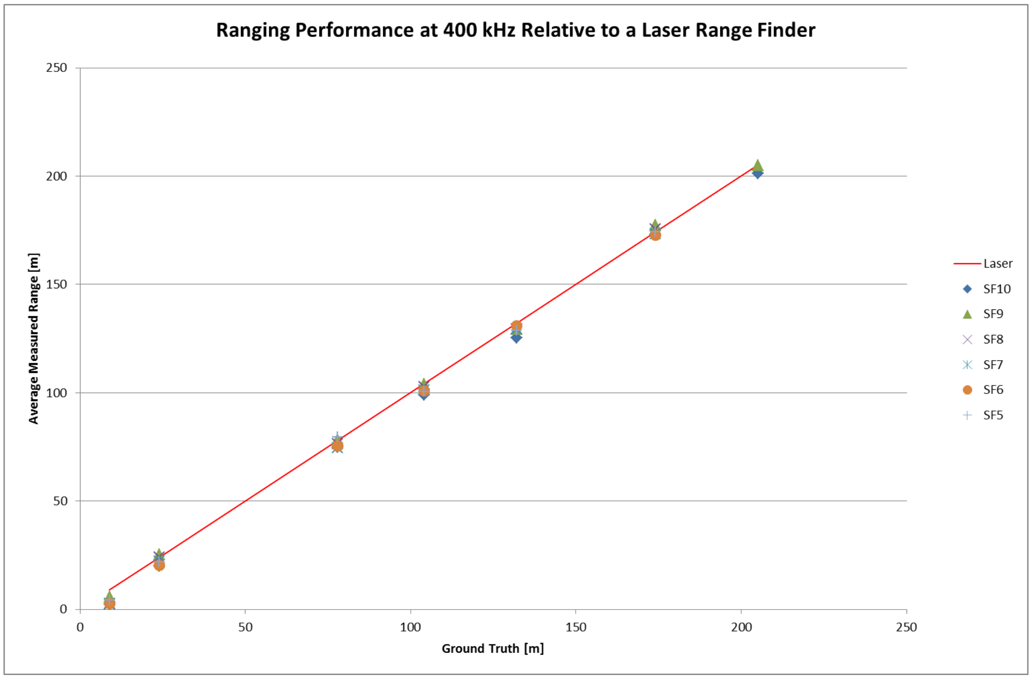

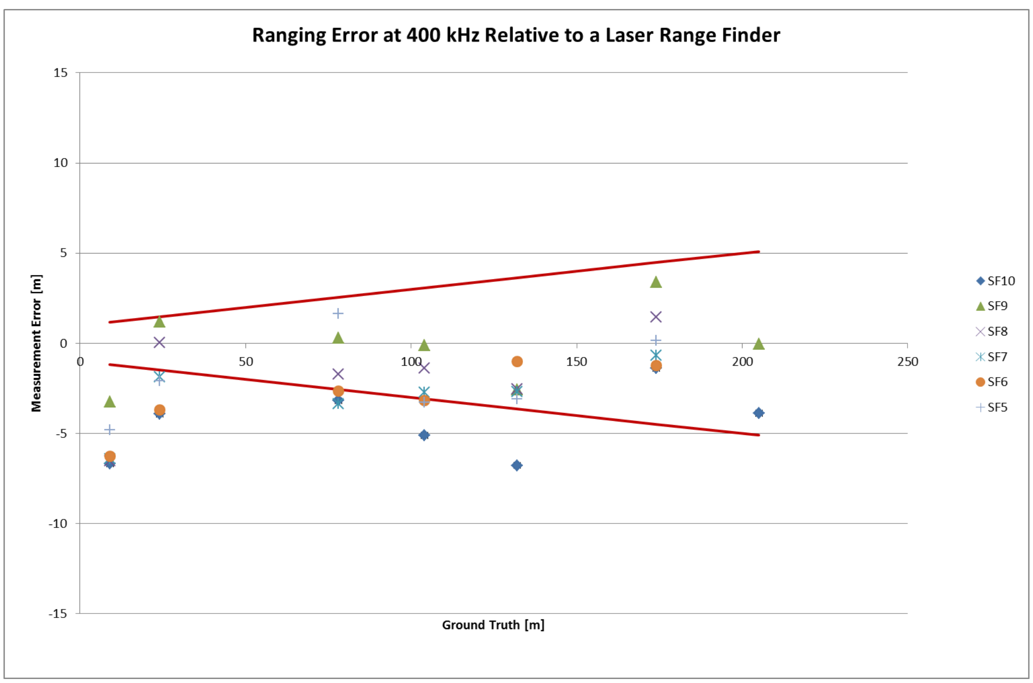

Figure 17: 400 kHz Bandwidth Ranging Accuracy for all Spreading Factors
Top: RTToF Range versus Laser Range Finder
Bottom: RTToF Measurement Error versus Laser Range Finder Measurement Error

Similarly with 800 kHz measurement bandwidth, with the exception of the 10 m measurement, virtually all measurements are within the notional laser range finder measurement error and the spread of results at each distance is reduced:

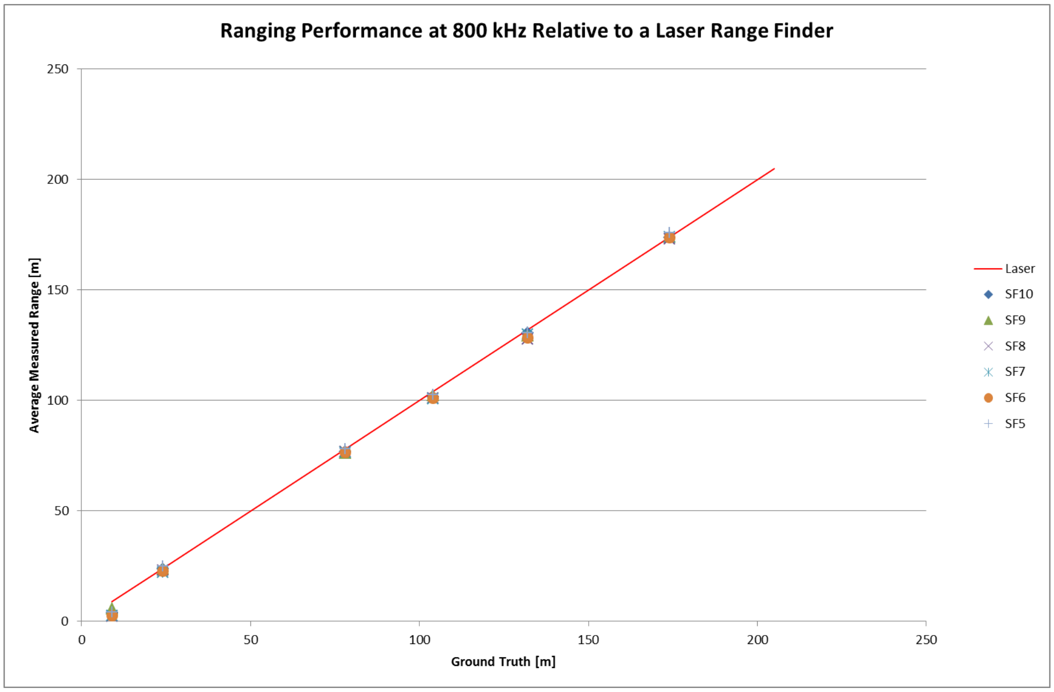

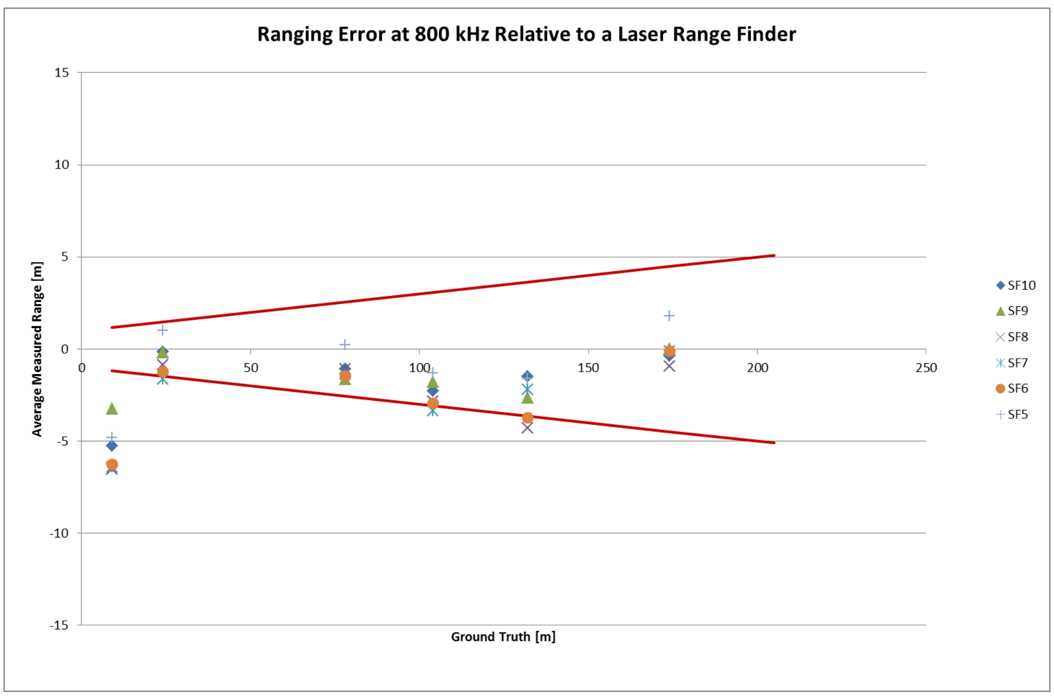

Figure 18: 800 kHz Bandwidth Measured Ranging Accuracy for all Spreading Factors
Top: RTToF Range versus Laser Range Finder
Bottom: RTToF Measurement Error versus Laser Range Finder Measurement Error

Finally, at 1600 MHz measurement bandwidth, the spread is even further reduced. The outlier at 10 m is now very clearly visible in both plots:

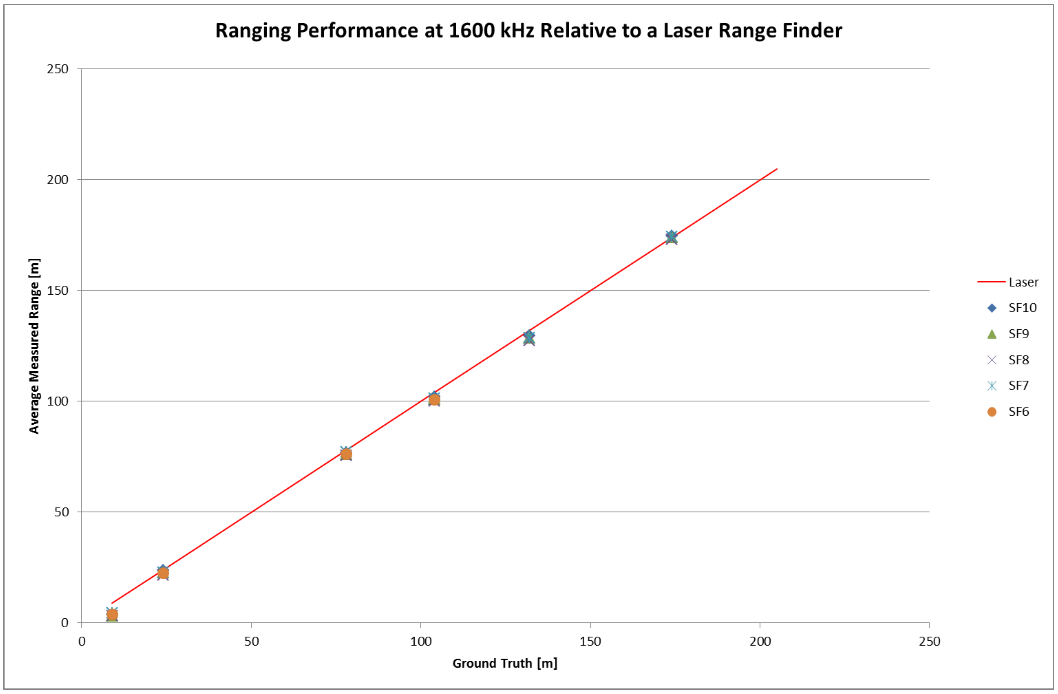

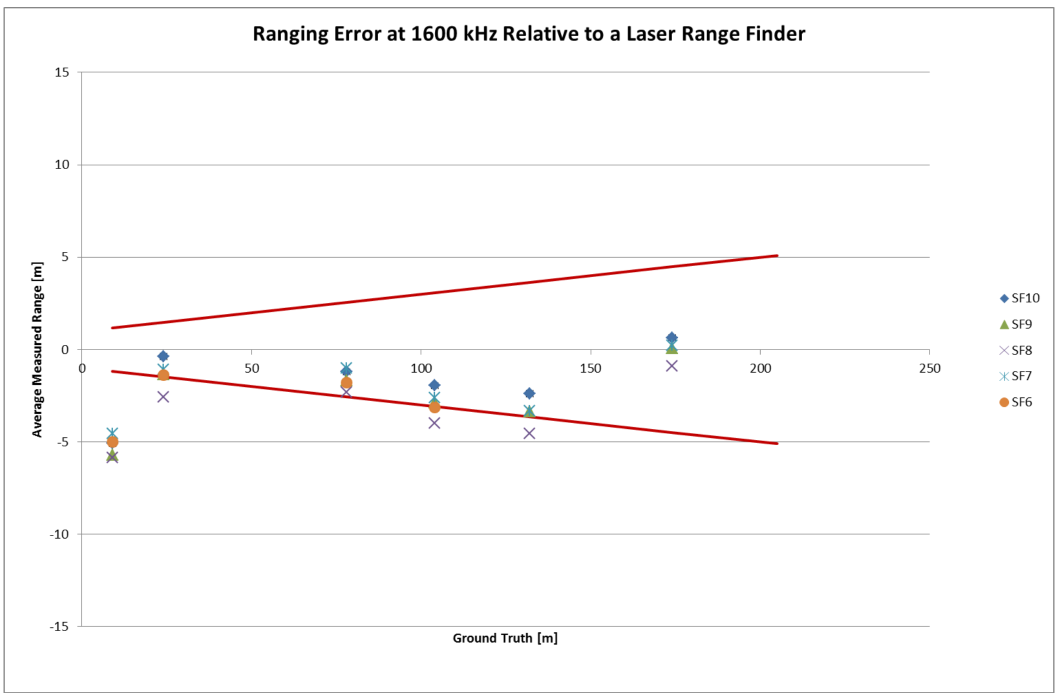

Figure 19: 1600 kHz Bandwidth Measured Ranging Accuracy for all Spreading Factors.
Top: RTToF Range versus Laser Range Finder
Bottom: RTToF Measurement Error versus Laser Range Finder Measurement Error

7.5 Accuracy and Number of Ranging Exchanges

Although we can attain measurement accuracy comparable to the laser range finder, in the previous examples 200 exchanges were considered. At low data rate (high spreading factor) and low bandwidth this can equate to seconds of exchange to perform a ranging operation.

If we consider a reduced number of exchanges, there is a trade-off between the number of exchanges and the resulting accuracy. In the example below, 400 ranging exchanges were obtained from 10 repetitions of the 40 channel-hopping sequences at SF9 1600 kHz. In the graph below each of the blue curves represents a new measurement sequence at the same distance (170 m). Each point is the absolute accuracy error, i.e. how far the average distance reported by the RTToF measurement is from ground truth.

In this plot we should consider the envelope of the plot as of most interest. The graph shows that the more ranging measurements are gathered, the more accurate the ranging becomes. The 1 meter accuracy (represented by green vertical line) is obtained after 80 ranging exchanges.

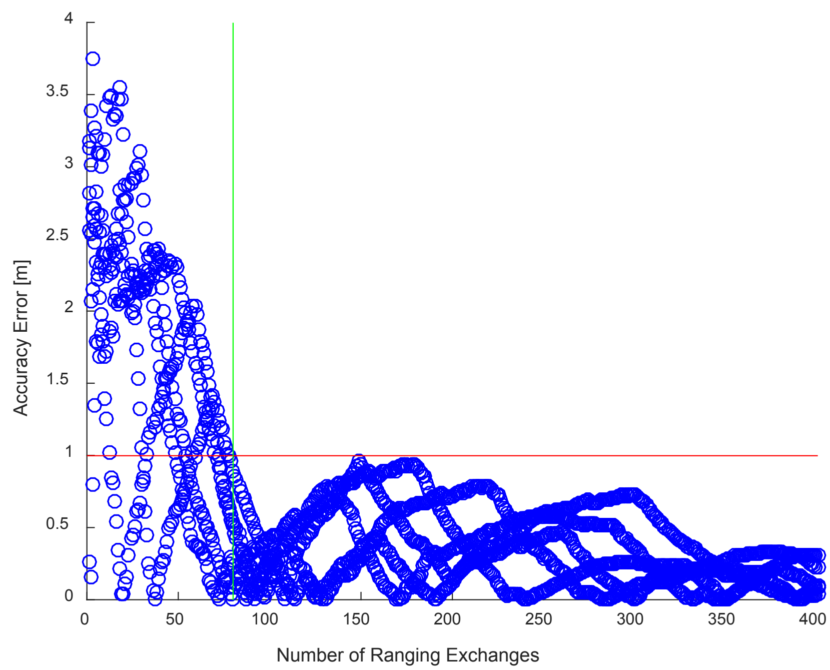

Figure 20: Absolute Ranging Accuracy at SF9 1600 kHz as Function of Number of Ranging Exchanges

7.6 Design Intuition

An individual ranging measurement on a single channel can be expected to have a ranging precision of approximately 1 m at high SF and high bandwidth. Aggregating 80 results over frequency-hopped channels will provide an accuracy of approximately 1 m at those high SF and high bandwidth settings.

In the broader context of link design trade-offs, this implies that there is a compromise to be struck between accuracy, time-on-air (equivalently energy consumption), and the range of the link. Optimization for a specific design target may be given by the following design considerations:

- Higher accuracy can be attained by increasing the number of measurements (see previous *Section 7.5* for more information on limitations) or increasing the spreading factor and bandwidth
- Lower time on air can be achieved by reducing the spreading factor and increasing bandwidth
- Longer range is possible by reducing the bandwidth and increasing the spreading factor

Recalling that spreading factor and modem bandwidth are the main variables available to the designer, the following graphic illustrates this design compromise for a given LoRa modem setting:

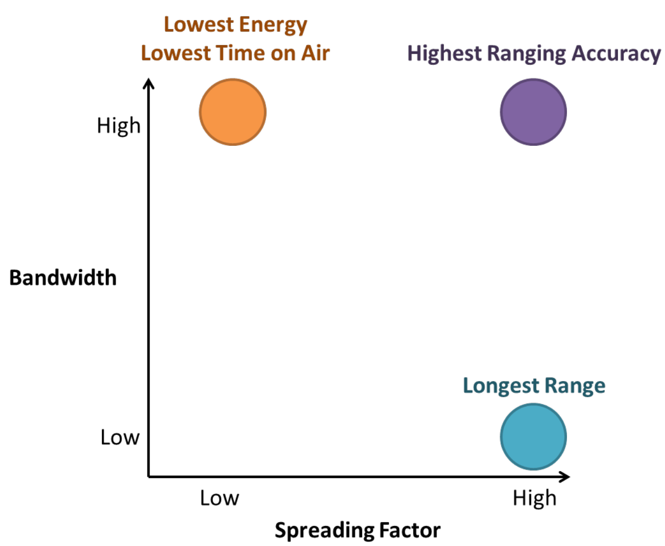

Figure 21: Selecting the Best LoRa Modem Configuration for a Given Application

8 Short Range Result Processing

As we saw in the preceding section, at short distance (below 20 m) the ranging results exhibit some non-linearity in the form of an increase in the observed gradient as a function of distance. This means that very short distances will be underestimated or could even become negative at very short range.

To resolve this, a correction is applied to measured distances below approximately 20 m. Although beyond the scope of this Application Note, curve fitting is applied to short range results. After a ranging measurement campaign, it appears that the best choice for the regression was an exponential basis function.

The following example shows the principle of operation of such a correction as pseudo-code. Corrections are expected to be application and antenna specific, so please consult the SX1280 application software for an example of a practical implementation [8].

```
IF measuredDistance <= 18.5 m

      displayDistance = EXP( ( measuredDistance +2.4917 ) / 7.2262 )
ELSE
      displayDistance = measuredDistance
END
```

Where `measuredDistance` is the distance reported by the ranging measurement and the `displayDistance` is the corrected value reported to the user. The original measurement results and a corrected example are shown in the graph below and compared with the ideal x = y curve.

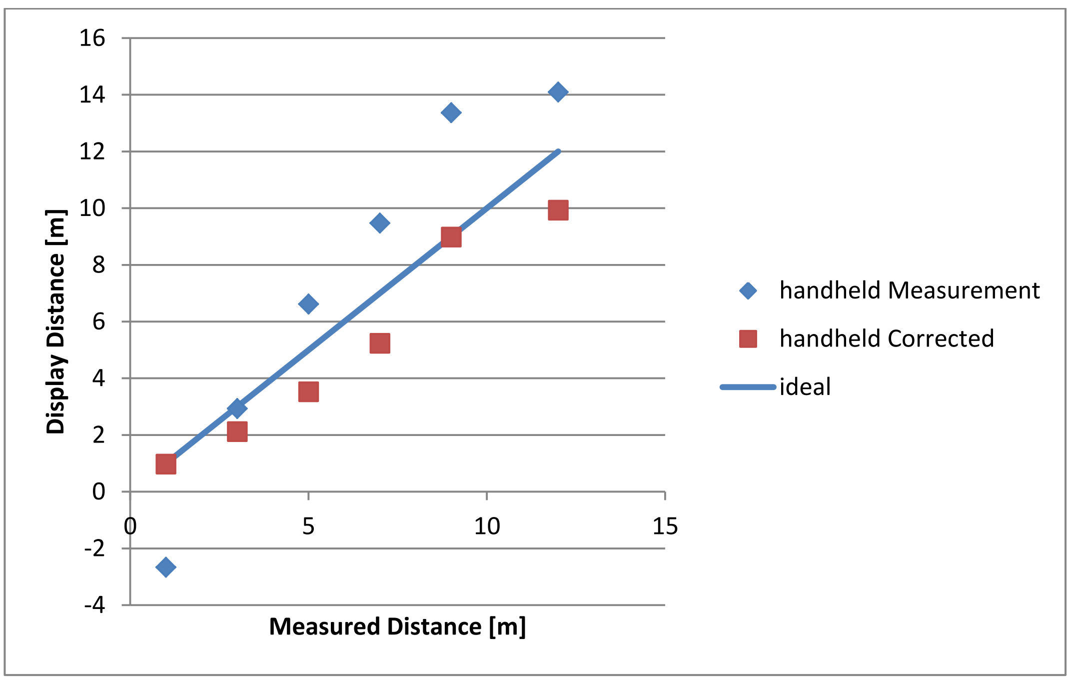

Figure 22: Illustrative Example of Short Range Measurement Error Correction

9 Conclusion

All of the steps required to calibrate both the fixed and variable timing offsets that could corrupt SX1280 RTToF measurement have been presented. In a practical peer-to-peer ranging system with a basic frequency-hopping protocol a ranging precision of less than 0.5 m was found in an ideal (cable) single frequency channel, rising to 1 m in a line of sight radiated configuration.

Accuracy of approximately 1 m is possible in SF9 with 1600 kHz bandwidth, based upon an average of 80 ranging exchanges over 40 frequency-hopped channels.

10 References

[1] Andreas F. Molisch, in *Wireless Communications*, Second Edition, 2011, John Wiley & Sons Ltd. ISBN: 978-0-470-74187-0, p. 27-31

[2] INTERNATIONAL STANDARD ISO/IEC 24730-5 Information technology, Real-time locating systems (RTLS) - Part 5: Chirp spread spectrum (CSS) at 2.4 GHz air interface. First edition 2010-04-01

[3] SX1280 Datasheet, Semtech Corporation
http://www.semtech.com/images/datasheet/sx1280_81.pdf

[4] Bartlett, in *Essentials of Positioning and Location Technology* Cambridge April 2013, p. 132-136

[5] Lanzisera et al, in *RF Time of Flight Ranging for Wireless Sensor Network Localization*, Fourth Workshop on Intelligent Solutions in Embedded Systems (WISES'06), Austria, June 30th, 2006
http://robotics.eecs.berkeley.edu/~pister/publications/2006/Lanzisera%20RF%20TOF.pdf

[6] Bresser 800 m LR Laser Range Finder Manual
https://www.bresser.de/out/media/51fc6c7abb2ee381d00b4c470b50f3f2.pdf

[7] Lois P. Sicking, in *Rangefinder Comparison*, US Forest Service Febuary 1998
https://www.fs.fed.us/eng/pubs/html/98241307/98241307.html

[8] SX1280 MBED Reference Code
https://developer.mbed.org/components/SX1280RF1ZHP/

Important Notice

Contact Information

Semtech Corporation
Wireless & Sensing Products
200 Flynn Road, Camarillo, CA 93012
E-mail: sales@semtech.com
Phone: (805) 498-2111, Fax: (805) 498-3804
www.semtech.com